# Analysis and Application of Advanced Control Strategies to a Heating Element Nonlinear Model



2017 J. Phys.: Conf. Ser. 783 012027

(http://iopscience.iop.org/1742-6596/783/1/012027)

IOP Conf. Series: Journal of Physics: Conf. Series **783** (2017) 012027 doi:10.1088/1742-6596/783/1/012027

# Analysis and Application of Advanced Control Strategies to a Heating Element Nonlinear Model

**C. Turhan[1], S. Simani[2], I. Zajic[3], G. Gokcen Akkurt[1]**

[1]Izmir Institute of Technology, Department of Mechanical Engineering, Gulbahce Campus, Urla – 35430 Izmir, Turkey. [2]Department of Engineering, University of Ferrara. Via Saragat 1E, 44122 Ferrara (FE), Italy. [3]Control Theory and Applications Centre, Coventry University, Coventry, United Kingdom.

E-mail: cihanturhan@iyte.edu.tr, silvio.simani@unife.it, zajici@uni.coventry.ac.uk

**Abstract.** This paper presents the design of different control strategies applied to a heating element nonlinear model. The description of this heating element was obtained exploiting a data–driven and physically meaningful nonlinear continuous–time model, which represents a test–bed used in passive air conditioning for sustainable housing applications. This model has low complexity while achieving high simulation performance. The physical meaningfulness of the model provides an enhanced insight into the performance and functionality of the system. In return, this information can be used during the system simulation and improved model–based and data–driven control designs for tight temperature regulation. The main purpose of this study is thus to give several examples of viable and practical designs of control schemes with application to this heating element model. Moreover, extensive simulations and Monte–Carlo analysis are the tools for assessing experimentally the main features of the proposed control schemes, in the presence of modelling and measurement errors. These developed control methods are also compared in order to evaluate advantages and drawbacks of the considered solutions. Finally, the exploited simulation tools can serve to highlight the potential application of the proposed control strategies to real air conditioning systems.

## 1. Introduction

Buildings are responsible for approximately 40% of the total energy consumption in the entire world [1, 2]. In developed countries, 50% of this energy is used for air conditioning purposes in buildings [3].

Energy control of the air conditioning systems is crucial to satisfy thermal comfort including relative humidity and temperature which is the primary variable in controlling air conditioners. Heating Elements (HEs) play an essential role for supplying treated air with specified temperature to the conditioned space in the buildings. Building control strategies require extensive computational requirements and necessity of a mathematical model of the HE system. Since the mathematical model is a description of the system behaviour, accurate modelling for a complex nonlinear system is very difficult to achieve in practice.

The HE system is a nonlinear system in the control of view, therefore, most of temperature control systems use conventional controllers like on–off controllers, including standard PID or PI regulators for its relative simplicity. However, these controllers do not always produce fast response and suffer the problem of overshoot, large settling time. Moreover, the tuning of the conventional controllers is difficult [4]. For example, when HE systems include bilinear

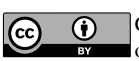

terms depending on temperature and mass flow rate, advanced control systems can be needed to optimise the design problem. To this aim, Artificial Intelligence (AI) has been applied to temperature control due to substantial advantages of applicability to nonlinear systems with unknown or partially known dynamics [5].

In the last years, AI based methods, namely, Fuzzy Logic (FL), Adaptive Neuro–Fuzzy Inference System (ANFIS), Artificial Neural Network (ANN) and Model Predictive Controllers (MPC) have been considered for trying to achieve more comfortable environments in buildings, see *e.g.* [6, 7, 4, 8, 9, 10, 11, 12]. These controllers have better advantages compared to the conventional ones. For instance, the paper [11] addressed the implementation of a MPC for the temperature control of a building. The controller achieved a saving of $17 - 24\%$ compared to a weather–compensated control technique. Similarly, the work [3] shows the development of a MPC algorithm to maintain the thermal comfort resulting in 28% of heating energy savings. In addition to the MPC, FL controllers were studied to control the temperature in heating systems by some authors [10, 9]. The authors demonstrated that the nonlinearity of the system can be easily managed with a FL controller, thus obtaining good performances. The paper [4] compared PID and ANN controllers. The authors designed an ANN controller feeding–back the air conditioning system. The ANN controllers allowed for shorter rise time and zero overshoot of the controller output. Although ANNs are widely used in the literature [8], some researchers studied more efficient control techniques based on the ANFIS tool, with the advantages of both ANN and FL [10, 5, 13]. In particular, the paper [13] used ANFIS controller effectively to model nonlinear functions to obtain thermal comfort conditions including temperature and relative humidity. The authors observed that maximum absolute error was less than $0.015\,^oC$ for temperature control. Adaptive controllers help the heating systems to maintain thermal comfort, while enhancing energy savings, as shown *e.g.* in [3]. Note finally that the increased popularity of AI control techniques for building temperature control is incontrovertible; however most of them do not give a comparison with extensive simulations.

This paper is focussed on the design of different control strategies with application to the HE nonlinear model developed by one of the same authors in [14]. The simulations and the comparisons with the achieved performances have been implemented in the Matlab and Simulink environments.

The rest of the paper is organised as follows. The heating element system is summarised in Section 2. Section 3 provides the control methods. The achieved results are summarised in Section 4. Comparisons among the different control methods and their performances with respect to measurements and modelling errors are also investigated and discussed. Finally, Section 5 concludes the paper by summarising the main achievements of the work, and providing some suggestions for further research topics.

## 2. Heating Element Model Description

The HE is a large test–bed system for testing and modelling of Phase Change Materials (PCM) used in the passive air conditioning for sustainable housing applications. The test–bed is installed in a large indoor space with approximately constant ambient temperature, as shown in Fig. 1.

The inputs of the HE system are the speed and temperature of air, $v$ $[m\,s^{-1}]$ and $T_i$ $[K]$, respectively, passing through the tested PCM. The output is the outlet temperature $T_o$ $[K]$. The air is conditioned by passing through the considered HE, which is connected in a downstream series connection with a cooling unit. The schematic diagram of the heating element installed in the supply duct is represented in Fig. 2. The measurements of $v$, $T_i$, and $T_o$ are taken from the centre of the cross sectional area of the supply duct.

The HE system is mainly described by 3 nonlinear differential relations. The energy balance equations for the HE, the control volume of air surrounding the HE and the adjacent duct walls

are represented by Eqs. (1), (2), and (3), respectively:

$$C_h \frac{dT_h(t)}{dt} = q(t) - (UA)_h \left[T_h(t) - T_o(t)\right] \quad (1)$$

$$0 = (UA)_h \left[T_h(t) - T_o(t)\right] + \\ -v(t)\,\rho_a\,A_a\,c_a\,\left[T_o(t) - T_i(t)\right] + \\ -(UA)_{int}\left[T_o(t) - T_w(t)\right] \quad (2)$$

$$C_w \frac{dT_w(t)}{dt} = (UA)_{int}\left[T_o(t) - T_w(t)\right] + \\ -(UA)_{ext}\left[T_w(t) - T_a(t)\right] \quad (3)$$

where $C_h$ $[J/K]$ is the thermal capacity of the heating element, $C_w$ $[J/K]$ the thermal wall capacity (insulated plywood), $c_a$ [J/kgK] is the air specific heat capacity, $A_a$ $[m^2]$ denotes the cross sectional area of the duct, $\rho_a$ $[kg/m^3]$ is the air density.

**Figure 1.** The HE test–bed.

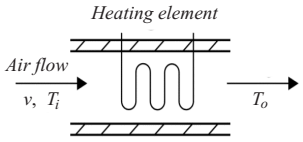


**Figure 2.** HE schematic diagram.

The heat transfer coefficient is denoted by $U$ $[J/m^2K]$, whilst the products of the heat transfer coefficient by the efficient surface area, $A$ $[m^2]$, through which the heat is transmitted are denoted with $(UA)_h$ $[J/K]$ (when referred to the HE), $(UA)_{int}$ $[J/K]$ (with reference to the inner duct wall), and $(UA)_{ext}$ $[J/K]$ (for the the outer duct wall). The mean temperature of the heating element and wall temperature are represented by $T_h(t)$ $[K]$ and $T_w(t)$ $[K]$, respectively. $q(t)$ is the power supplied by the heating element. Eq. (2) assumes that the passing air has negligible thermal capacity, hence the left hand side of Eq. (2) equals to zero. Note finally that the HE model was described in more detail in [14].

## 3. Control Scheme Designs

The general description of the dynamic model of the HE can be represented by the nonlinear dynamic function $P$:

$$y = P\,(u, t) \quad (4)$$

where $y$ is the process output, $u$ is its input, and $t$ is the time. The control strategy applied to the HE should determine the control input such that the controlled process is able to track a given reference $r(t)$ [14].

It can be shown that the overall dynamic behaviour of the HE process (4) can be approximated with very good accuracy by a product of 2 second–order continuous–time transfer functions, as shown in [14]. On the other hand, the continuous–time linearised state–space description of the HE nonlinear process (4) is described by the system (5):

$$\begin{cases} \dot{x}(t) &= A\,x(t) + B\,u(t) \\ y(t) &= C\,x(t) \end{cases} \tag{5}$$

with $x \in \Re^4$. The control input is represented by the mass flow rate speed $u(t) = v$, and the measured output is $y(t) = T_o$. In general, Heating, Ventilation, and Air Conditioning (HVAC) systems have a second input $T_i$, *i.e.* the air flow input temperature, which is considered as a measurable disturbance, $d$.

This paper recalls different control strategies including the standard PID controller as well as AI techniques, such as fuzzy logic, adaptive, model predictive controllers, which are used for the regulation of the outlet temperature of the HE system. These methodologies are briefly outlined in the following subsections.

### *3.1. PID Controller Design*

Standard PID regulators are the most commonly used feedback controllers for industrial processes. The control logic is based on the computation of the error $e(t)$ between the desired and the measured values of the output, *i.e.* $e(t) = r(t) - y(t)$, which is fed back to the system after proportional, integral and derivative operations [15]. In this way, the continuous–time control law of the PID regulator is described by Eq. (6):

$$u(t) = K_p\,e(t) + K_i \int_0^t e(\tau)\,d\tau + K_d \frac{de(t)}{dt} \tag{6}$$

where $K_p$, $K_i$, $K_d$ are the PID proportional, integral, and derivative gains. The optimal selection of this gains is performed by using the automatic tuning algorithm in the Simulink environment that balances the performance (response time) and the robustness (stability margins) of the controlled system [16]. The PID automatic tuning Simulink toolbox uses the linearised model (5) of HE system.

### *3.2. Fuzzy Controller Design*

Fuzzy Logic Controllers (FLCs) are extensively used in processes where the system dynamics are either very complex or exhibit highly nonlinear characteristics [10]. The controller design approach relies on the identification of transparent rule–based Takagi–Sugeno (TS) fuzzy models using an Adaptive Neuro–Fuzzy Inference System (ANFIS) tool implemented in the Simulink toolbox [17].

The TS fuzzy model consists of a set of rules $R_i$, where the consequents are deterministic functions $f_i$:

$$R_i : IF\,x\,is\,A_i\,THEN\,u_i = f_i(x) \tag{7}$$

with $i = 1, 2, \ldots, K$ and $K$ is the number of clusters or rules of the rule–based system, $x$ represents the vector of the *antecedent* variables, and $u_i$ describes the *consequent* output. $A_i$ represents the antecedent fuzzy set of the $i$–th rule, defined by its (multivariable) membership function $\mu_{A_i}(x) \rightarrow [0, 1]$ The function $f_i$ is represented by suitable parametric models, whose structure remains equal in all rules, whilst the parameters can vary. A parametrisation in affine form is usually exploited, and described by Eq. (8):

$$u_i = a_i\,x + b_i \tag{8}$$

where the vector $a_i$ and the scalar $b_i$ are the $i$–th submodel parameters. The vector $x$ contains a suitable number $n$ of delayed samples of the model inputs and output. In this way, the product $a_i\,x$ represents an Auto–Regressive eXogenous (ARX) parametric dynamic model of order $n$.

The final output $u$ of the TS fuzzy model is the weighted average of all rule outputs, computed as:

$$u = \frac{\sum_{i=1}^{K} \mu_{A_i}(x)\, y_i(x)}{\sum_{i=1}^{K} \mu_{A_i}(x)} \tag{9}$$

The modelling approach used by ANFIS is similar to many system identification techniques. First, the TS fuzzy model structure described by the its order $n$, the form of the membership functions $\mu_{A_i}$ and the number of clusters $K$ are hypothesised. Next, the input–output data are used by ANFIS for training the TS model according to a chosen error criterion, thus determining the optimal values of the controller parameters $a_i$ and $b_i$ [17].

The paper considers also an alternative approach to ANFIS for the derivation of the controller fuzzy model, which is represented by the Fuzzy Modelling and Identification (FMID) toolbox developed in the Matlab environment [18]. Also in this case, the estimation of the controller prototype relies on the identification of rule–based fuzzy models and using the input–output data acquired from the controlled process. This method exploits Takagi–Sugeno fuzzy models and employs the Gustafson–Kessel clustering method to divide the data into subsets with a common local linear (affine) behaviour [18].

The identified fuzzy controller is thus obtained by selecting an proper model structure $n$ and a number of clusters $K$. The FMID toolbox provides the parameters $a_i$, $b_i$ and the estimation of the membership functions $\mu_{A_i}$ of the optimal controller minimising the tracking error $e(t)$, *i.e.* the difference between the reference signal $r(t)$ and the measured output $y(t)$.

Note finally that the fuzzy controller in the form of Eq. (9) is described by a discrete–time input–output model, which is connected to the controlled continuous–time nonlinear system of Eq. (4) using Digital–to–Analog (D/A) and Analog–to-Digital (A/D) converters.

### *3.3. Adaptive Control Design*

The adaptive control method exploited in this paper is based on the on–line identification of a second order discrete–time transfer function of an ARX time–varying model in the form:

$$G(z) = \frac{b_1\, z^{-1} + b_2\, z^{-2}}{1 + a_1\, z^{-1} + a_2\, z^{-2}} \tag{10}$$

whose parameters are recursively estimated at each sampling time $t_k = k\,T$, with $k = 1, 2, \ldots, N$, $N$ the number of samples, and $T$ the sampling interval. $z$ represents the unit advance operator. The parameters in (10) are estimated using the Recursive Least–Square Method (RLSM) with directional forgetting factor [19].

The synthesis of the adaptive control law is derived using a modified Ziegler–Nichols criterion, in the form of Eq. (11):

$$\begin{aligned} u_k \;=\; & q_0\, e_k + q_1\, e_{k-1} + q_2\, e_{k-2} + \\ & + (1-\gamma)\, u_{k-1} + \gamma\, u_{k-2} \end{aligned} \tag{11}$$

where $e_k$ is the tracking error $e(t)$ at the sampling time $t_k$, $u_k$ the control signal $u(t)$ at the sampling time $t_k$, whilst $q_0$, $q_1$, $q_2$, and $\gamma$ are the time–varying controller parameters, which are calculated by solving a Diophantine equation that leads to the following relations [19]:

$$\begin{aligned} q_0 &= \tfrac{1}{b_1}\,(d_1 + 1 - a_1 - \gamma)\,, \qquad \gamma = q_2\,\tfrac{b_2}{a_2} \\ q_1 &= \tfrac{a_2}{b_2} - q_2\left(\tfrac{b_1}{b_2} - \tfrac{a_1}{a_2} + 1\right), \quad q_2 = \tfrac{s_1}{r_1} \end{aligned} \tag{12}$$

where $r_1 = (b_1 + b_2)\left(a_1\, b_2\, b_1 - a_2\, b_1^2 - b_2^2\right)$ and $s_1 = a_2\,(\,(b_1 + b_2)\,(a_1\, b_2 - a_2\, b_1) + +b_2\,(b_1\, d_2 - b_2\, d_1 - b_2)\,)$. It is assumed that the final closed loop model has a behaviour similar to a second–order continuous time system with characteristic polynomial $s^2 + 2\,\delta\,\omega\,s + \omega^2$, where $\delta$ and $\omega$ represent its damping factor and natural frequency, respectively. In this case, if $\delta \leq 1$, $d_1 = -2\,e^{-\delta\,\omega\,T}\,\cos\left(\omega\,T\sqrt{1-\delta^2}\right)$ and $d_2 = e^{-2\,\delta\,\omega\,T}$.

Both the on–line identification procedure and the adaptive controller parameter computation are implemented in the self–tuning controller Simulink library [19]. In this way, the sampled output $y_k$ of the time–varying ARX model (10) should follow the sampled reference signal $r_k$ when regulated by the control law (11). Note finally that, also in this case, the adaptive controller (11) is connected to the continuous–time nonlinear system (4) using the D/A and A/D converters.

### *3.4. Model Predictive Control Design*

Model Predictive Control (MPC) relies on dynamic models of the process, most often linear models obtained by system identification or linearisation of a nonlinear plant. The main advantage of MPC is the fact that it allows the current sampling time to be optimised, while keeping future sampling times in account. This is achieved by optimising a finite time–horizon, but only implementing the current sampling time. MPC has the ability to anticipate future events and can take control actions accordingly. PID controllers do not have this predictive ability. MPC is nearly universally implemented as a digital control.

MPC is based on iterative, finite–horizon optimisation of the plant model. At the sample $k$ ($k = 1, 2, \ldots, N$) the current plant output is sampled and a cost minimising control strategy is computed (via a numerical minimisation algorithm) for a relatively short time horizon in the future: $[k, k + N_p]$. Specifically, an online calculation is used to explore state trajectories that emanate from the current state and find (via the solution of Euler–Lagrange equations) a cost–minimising control strategy until time $k + N_p$. Only the first step of the control strategy is implemented, then the plant state is sampled again and the calculations are repeated starting from the new current state, yielding a new control and new predicted state path. The prediction horizon keeps being shifted forward and for this reason MPC is also called receding horizon control. Although this approach is not optimal, in practice it has given very good results [20].

An example of a cost function $J$ for optimisation is given by:

$$J = \sum_{k}^{k+N_p} w_{y_k}\,(r_k - y_k)^2 + \sum_{k}^{k+N_c} w_{u_k}\,\Delta u_k^2 \tag{13}$$

where $w_{y_k}$ the weighting coefficient reflecting the relative importance of the monitored output, and $w_{u_k}$ the weighting coefficient penalising relative big changes in $u_k$, with $\Delta u_k = u_k - u_{k-1}$. $N_p$ represents the prediction horizon, whilst $N_c$ the control horizon.

Note finally that the discrete–time MPC design is performed by using the MPC toolbox in the Simulink environment, which computes a linearisation of the HE nonlinear model (5). The discrete–time MPC is thus connected to the continuous–time nonlinear system of Eq. (4) using the D/A and the A/D converters. The MPC Simulink toolbox uses the linearised model (5) of HE system.

## 4. Simulation Results

This study exploits the 5 different control methods described in the previous subsections to regulate the outlet temperature of the HE nonlinear system. The simulations are performed in the Simulink environment and the toolboxes described above. The achieved results are compared

in terms of settling time $T_s$, maximum overshoot $S\%$ and Mean Sum of Squared Errors (MSSE), defined as:

$$MSSE\% = 100 \sqrt{\frac{\sum_{k=1}^{N} (r_k - y_k)^2}{\sum_{k=1}^{N} r_k^2}} \tag{14}$$

The standard control strategy for HVAC systems uses a classic PI regulator, whose complete structure is recalled in Section 3.1 [14]. The optimal proportional and integral gains are determined using the automatic PID tuning procedure and settled to $K_p = 22$ and $K_i = 36$, respectively.

Fig. 3 shows the reference signal $T_o$ (blue continuous line) of test–bed in Fig. 1 and the process output (red dashed line) controlled by the PI regulator (6), as shown in Fig. 4. The settling time achieved by the PI controller is $T_s = 2.92s.$, with an overshoot of $S\% = 40.19\%$, which are computed by applying a step change in the reference output temperature from $39^oC$ to $40^oC$. Using the performance index (14), the tracking error is $MSSE\% = 0.51\%$.

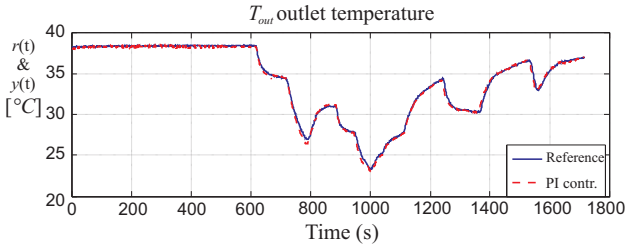


**Figure 3.** Outlet temperature controlled by the continuous–time PI regulator.

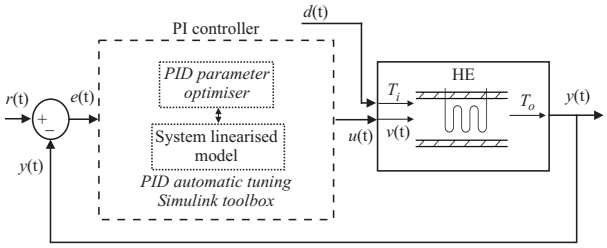


**Figure 4.** Block diagram of the HE system controlled by the standard PI regulator.

Standard industrial controllers, such the PID of Section 3.1, are quite simple and have the benefit of quite straightforward implementation. However, when applied to the control of HE systems, the control laws are not efficient, thus leading to possible high maintenance costs. Therefore, advanced controllers are exploited to reduce energy consumption and enhance thermal comfort.

With reference to the strategies described in Section 3.2, fuzzy identification is used to derive the models of the controllers by exploiting the so–called model reference control approach [21]. For this purpose, the PI regulator of Fig. 1 represents the reference controller for the generation of the data used by the identification strategy proposed described in Section 3.2. In this way, the fuzzy controller parameters are identified such that the performances in terms of tracking error $e(t)$ are optimised.

In particular, with reference to the TS fuzzy controller derived with the ANFIS tool, a sampling interval $T = 0.1s.$ is exploited. Moreover, the fuzzy controller (9) uses a number

$K = 3$ of Gaussian membership functions, with a number of delayed inputs and output $n = 1$. The antecedent vector is thus $x = [e_k, e_{k-1}, u_{k-1}]$. The achieved performances of the controller obtained with the ANFIS tool are shown in Fig. 5, whilst its implementation is sketched in Fig. 6.

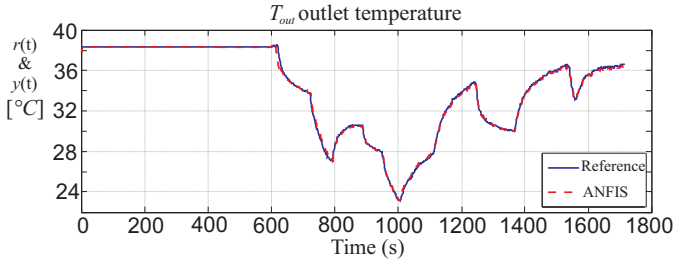


**Figure 5.** Outlet temperature controlled by the fuzzy controller obtained via the ANFIS tool.

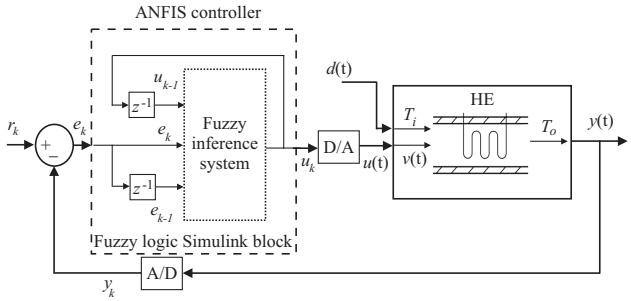


**Figure 6.** Block diagram of the HE system controlled by the ANFIS fuzzy regulator.

Fig. 5 highlights that fuzzy regulator performs slightly better than the standard PI controller. In this case, the settling time is $T_s = 3.05s.$, with an overshoot $S\% = 41.66\%$, and an $MSSE\% = 0.47\%$. .

Using the same data from the PI reference regulator, a second fuzzy controller (9) has been estimated using the FMID tool, with a number of clusters $K = 3$, a number of delays $n = 2$, and the antecedent vector $x = [u_{k-1}, u_{k-2}, r_k, r_{k-1}, y_k, y_{k-1},]$. The FMID tool provides also the optimal estimate of the shapes of the membership functions $\mu_{A_i}$. The implementation scheme is represented in Fig. 7, and the results of this fuzzy controller are shown in Fig. 8. Note that the high overshoot at the beginning of the simulation in Fig. 8 is due to the initial conditions of the delay blocks of the fuzzy controller represented in Fig. 7 that are zero.

Fig. 8 highlights that the reference signal is tracked with good accuracy, with a $MSSE\% = 0.09\%$. In this case, the settling time is $T_s = 3.15s.$ with a maximum overshoot $S\% = 41.25\%$.

On the other hand, by considering the on–line procedure recalled in Section 3.3, Fig. 9 shows the tracking capabilities of the adaptive controller (11). Its time–varying parameters have been obtained via the relations (12) with the damping factor and the natural frequency $\delta = \omega = 1$. The adaptive controller implementation using the Self Tuning controller Simulink Library (STCSL) is represented in Fig. 10.

The settling time of the HE system output with the adaptive controller is $T_s = 3.16s.$, and the overshoot is $S\% = 42.87\%$. The tracking error is $MSSE\% = 5.97\%$.

Finally, with reference to the MPC strategy recalled in Section 3.4, the reference and the monitored output signals are depicted in Fig. 11. Its implementation is sketched in Fig. 12.

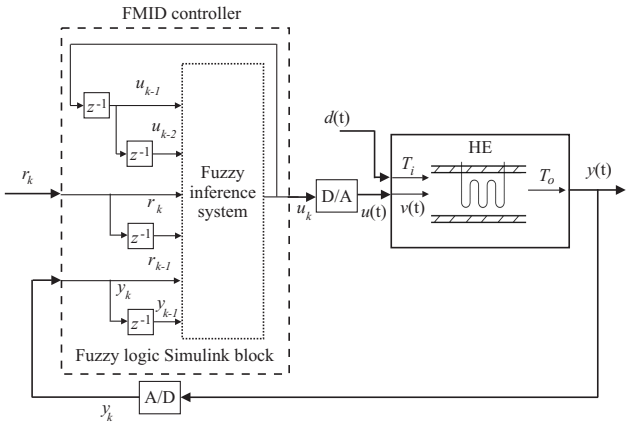


**Figure 7.** Block diagram of the HE system controlled by the FMID fuzzy regulator.

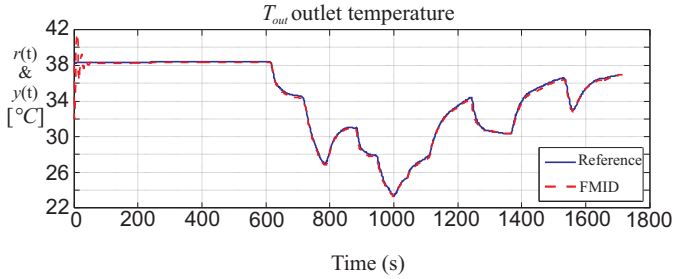


**Figure 8.** Outlet temperature controlled by the fuzzy controller estimated by the FMID tool.

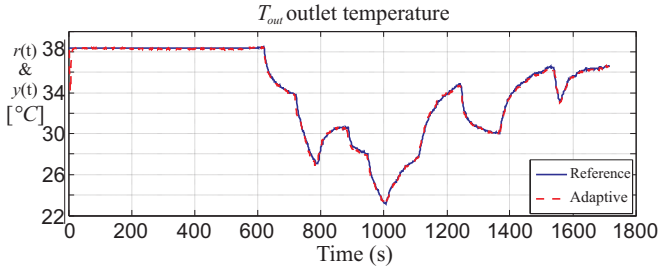


**Figure 9.** Outlet temperature controlled by the adaptive controller.

The results shown in Fig. 11 have been achieved by using a prediction horizon $N_p = 10$ and a control horizon $N_c = 2$. The weighting parameters have been settled to $w_{y_k} = 0.1$ and $w_{u_k} = 1$, in order to reduce abrupt changes of the control input that would lead to higher energy consumption. In this case, the settling time is $T_s = 3.49s$. and the overshoot is 40.68%. The tracking error corresponds to $MSSE\% = 3.2\%$. The achieved results in terms of settling time, maximum overshoot and nominal $MSSE\%$ values are summarised in Table 1.

Note that the standard PI regulator leads to the best values of settling time and maximum overshoot, as its parameters are automatically tuned in the Simulink environment in order to optimise these indices, as recalled in Section 3.1. On the other hand, the best performance in terms of tracking error is obtained with the fuzzy controller estimated via the FMID tool recalled Section 3.2.

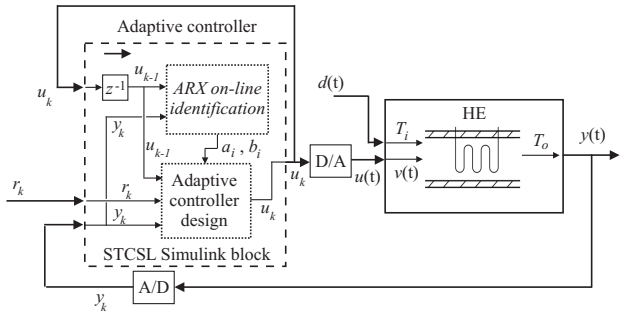


**Figure 10.** Block diagram of the HE system controlled by the adaptive regulator.

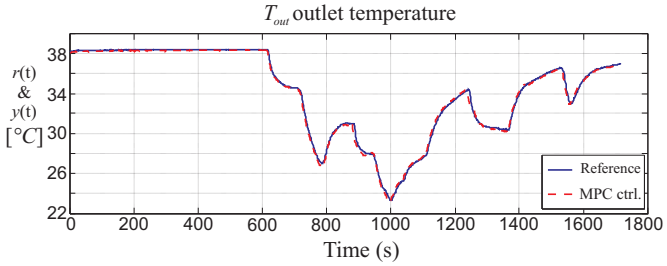


**Figure 11.** Outlet temperature controlled by the MPC.

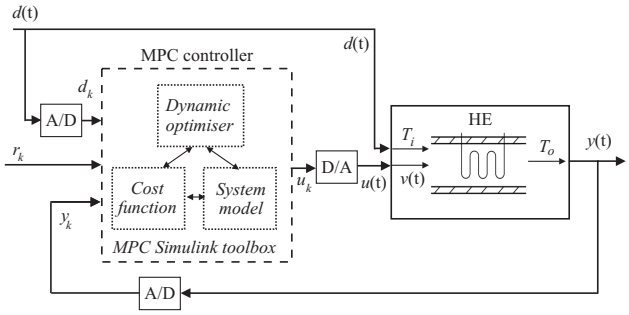


**Figure 12.** Block diagram of the HE system controlled by the MPC strategy.

**Table 1.** Comparison of the achieved performance in terms of $MSSE\%$.

| Controller type | Settling time $T_s$ | Overshoot $S\%$ | $MSSE\%$ nominal value |
|---|---|---|---|
| PI | $2.92s.$ | 40.19% | 0.51% |
| ANFIS | $3.05s.$ | 41.66% | 0.47% |
| FMID | $3.15s.$ | 41.25% | 0.094% |
| Adaptive | $3.16s.$ | 42.87% | 5.97% |
| MPC | $3.49s.$ | 40.68% | 3.19% |

The next section provides further results with some final comments regarding the robustness features of the proposed controllers applied to the HE nonlinear model.

*4.1. Parameter Sensitivity Analysis*

This section analyses the robustness features of the proposed controllers with respect to parameter variations. This analysis exploits the Monte–Carlo tool, as the control performance depends on the model–reality mismatch as well as on the input–output measurement errors. Therefore, the analysis has been performed by describing the HE model parameters as Gaussian stochastic processes with mean values corresponding to the nominal ones and standard deviations of $\pm 20\%$. The average, the best and the worst $MSSE$ index values have been computed with 100 Monte–Carlo runs, and summarised in Table 2.

**Table 2.** Comparison of the achieved performance in terms of $MSSE\%$.

| Controller type | $MSSE\%$ best case | $MSSE\%$ average case | $MSSE\%$ worst case |
|---|---|---|---|
| PI | 0.19% | 0.51% | 1.45% |
| ANFIS | 0.12% | 0.47% | 3.75% |
| FMID | 0.093% | 0.094% | 0.26% |
| Adaptive | 4.22% | 5.97% | 6.95% |
| MPC | 0.13% | 3.19% | 3.57% |

A few comments can be drawn here. When the modelling of the dynamic system can be taken into account, the MPC scheme is preferred, even if an optimisation procedure is required. However, in the case of a system with modelling errors, after a certain amount of off–line learning, the fuzzy–based estimation error can fall below the value of the MPC–based scheme, as shown for the controller estimated via the FMID tool. On the other hand, the FMID controller achieves the best control capabilities. The adaptive approach takes advantage of its improved features, as it is able to track possible variations of the controlled system, but with quite complicated and not straightforward design procedures. The fuzzy–based schemes rely on the learning accumulated from off–line simulations, but the training stage can be computationally heavy. Regarding the developed PI control strategy, it is rather simple and straightforward, even if the achievable performances are quite limited.

Finally, the results demonstrate also that the Monte–Carlo analysis is an effective tool for testing the suggested control methods. Moreover, in presence of uncertainty and modelling errors, this simulation tool seems to facilitate the validation of the considered control schemes for application to real HVAC cases.

## 5. Conclusion

In this study, different temperature control techniques were applied to a heating element nonlinear model, which can represent a part of a larger system used also for modelling phase change materials in passive air conditioning for sustainable housing applications. Simulations on the heating element nonlinear model and the Monte–Carlo analysis were the tools for assessing experimentally the properties of the designed control schemes, in the presence of modelling and measurement errors. The proposed control solutions relied on standard PID, fuzzy, adaptive, and model–predictive control strategies. The achieved results showed that these control schemes can be successfully used for the regulation of the temperature of the heating element system. Moreover, the proposed comparisons among the different control strategies highlighted also that the suggested control solutions can be promising for the real building control applications. Further studies will try to extend the developed schemes to the control of more advanced thermal comfort parameters, such as the relative humidity and the air flow.

## References

[1] N. Payam, J. Fatemeh, M. T. Mohammad, G. Mohammad, and M. A. Muhd Zaimi, "A global review of energy consumption, $CO_2$ emissions and policy in the residential sector (with an overview of the top ten $CO_2$ emitting countries)," *Renewable and Sustainable Energy Reviews*, vol. 43, pp. 843–862, March 2015. DOI: 10.1016/j.rser.2014.11.066.

[2] Y. Xing, N. Hewitt, and P. Griffiths, "Zero carbon buildings refurbishment – A hierarchical pathway," *Renewable and Sustainable Energy Reviews*, vol. 15, pp. 3229–3236, August 2011. DOI: 10.1016/j.rser.2011.04.020.

[3] D. Lindelof, H. Afshari, M. Alisafaee, J. Biswas, M. Caban, X. Mocellin, and J. Viaene, "Field tests of an adaptive, model–predictive heating controller for residential buildings," *Energy and Buildings*, vol. 99, pp. 292–302, May 2015. DOI: 10.1016/j.enbuild.2015.04.029.

[4] P. Kumar and K. P. Singh, "Comparative analysis of air conditional system using PID and neural network controller," *International Journal of Scientific and Research Publications*, vol. 3, pp. 1–6, August 2013. ISSN: 2250–3153. DOI: 10.1.1.415.2205.

[5] J. Moon, S. K. Jung, Y. Kim, and S. H. Han, "Comparative study of artificial intelligence–based building thermal control – Application of fuzzy, adaptive neuro–fuzzy inference system and artificial neural network," *Applied Thermal Engineering*, vol. 31, pp. 2422–2429, October 2011. DOI: 10.1016/j.applthermaleng.2011.04.006.

[6] A. I. Dounis and C. Caraiscos, "Advanced control systems engineering for energy and comfort management in a building environment – a review," *Renewable and Sustainable Energy Reviews*, vol. 13, pp. 1246–1261, August–September 2009. DOI: 10.1016/j.rser.2008.09.015.

[7] M. Krarti, "An overview of artificial intelligence–based methods for building energy systems," *Journal of Solar Energy Engineering*, vol. 125, pp. 331–342, August 2003. DOI: 10.1115/1.1592186.

[8] P. M. Ferreira, A. E. Ruano, S. Silva, and E. Z. E. Conceicao, "Neural networks based predictive control for thermal comfort and energy savings in buildings," *Energy and Buildings*, vol. 55, pp. 238–251, December 2012. DOI: 10.1016/j.enbuild.2012.08.002.

[9] M. He, W. J. Cai, and S. Y. Li, "Multiple fuzzy model–based temperature predictive control for HVAC systems," *Information Science*, vol. 169, pp. 155–174, January 2005. DOI: 10.1016/j.ins.2004.02.016.

[10] S. Soyguder and H. Alli, "An expert system for the humidity and temperature control in HVAC systems using ANFIS and optimization with Fuzzy Modelling Approach," *Energy and Buildings*, vol. 41, pp. 814–822, August 2009. DOI: 10.1016/j.enbuild.2009.03.003.

[11] S. Privera, J. Siroky, L. Ferkl, and J. Cigler, "Model predictive control of a building heating system: The first experience," *Energy and Buildings*, vol. 43, pp. 564–572, February–March 2011. DOI: 10.1016/j.enbuild.2010.10.022.

[12] J. Siroky, F. Oldewurtel, J. Cigler, and S. Privara, "Experimental analysis of model predictive control for an energy efficient building heating system," *Applied Energy*, vol. 88, pp. 3079–3087, September 2011. DOI: 10.1016/j.apenergy.2011.03.009.

[13] K. L. Ku, J. S. Liaw, M. Y. Tsai, and T. Liu, "Automatic control system for thermal comfort based on predicted mean vote and energy saving," *IEEE Transactions on Automation Science and Engineering*, vol. 12, pp. 378–383, Jan. 2015. DOI: 10.1109/TASE.2014.2366206.

[14] I. Zajic, M. Iten, and K. J. Burnham, "Modelling and data–based identification of heating element in continuous–time domain," *Journal of Physics: Conference Series*, vol. 570, no. 1, p. 012003, 2014. DOI: 10.1088/1742-6596/570/1/012003.

[15] K. J. Åström and B. Wittenmark, *Computer Controlled Systems: Theory and Design*. Englewood Cliffs, N.J. 07632: Prentice-Hall, third ed., 1990.

[16] K. J. Åström and T. Hägglund, *Advanced PID Control*. Research Triangle Park, NC 27709: ISA - The Instrumentation, Systems, and Automation Society, 2006. ISBN: 978–1–55617–942–6.

[17] J. S. R. Jang, "ANFIS: Adaptive–Network–based Fuzzy Inference System," *IEEE Transactions on Systems, Man., & Cybernetics*, vol. 23, pp. 665–684, May 1993.

[18] R. Babuška, *Fuzzy Modeling for Control*. Boston, USA: Kluwer Academic Publishers, 1998.

[19] V. Bobál, J. Böhm, J. Fessl, and J. Machácek, *Digital Self–Tuning Controllers: Algorithms, Implementation and Applications*. Advanced Textbooks in Control and Signal Processing, Springer, 1st ed., 2005.

[20] M. Nikolaou, *Advances in Chemical Engineering*, vol. 26, ch. Model predictive controllers: A critical synthesis of theory and industrial needs, pp. 131–204. Academic Press, 2001.

[21] M. Brown and C. Harris, *Neurofuzzy Adaptive Modelling and Control*. Prentice Hall, 1994.